IEICE Communications Express, Vol.13, No.6, 218–221

ComEX

LETTER

On signal detection parameters for energy detection based carrier sense in LPWANs

Shusuke Narieda [1, a)] **and Takeo Fujii**[2]

Abstract This study investigates the characteristics of signal detection parameters, such as target signal detection probability and false alarm probability of an energy detection based carrier sense, which can effectively avoid interferences in the same frequency band, in low power wide area networks (LPWANs). The aforementioned target probabilities strongly affect the characteristics of energy detection and its application, and revealing the characteristics that enhance the performance of energy detection based carrier sense is important. Two types of numerical example based analysis are presented from the viewpoints of signal detection and wireless networks. The analytical results show the presence of an optimal target false alarm probability.

Keywords: LPWAN, energy detection based carrier sense, target false alarm probability, target signal detection probability
Classification: Wireless communication technologies

1. Introduction

The concept of the Internet of Things (IoT) is widely spreading regardless of use in public facilities or commercial use, and it appears in several applications, such as industrial management [1], environmental monitoring [2], and smart cities [3]. Billions of end devices with physical sensors and wireless transceiver will be deployed in the real world for these IoT applications. Low power wide area networks (LPWANs) [4] could be the wireless infrastructure of such IoT applications because of their characteristics, that is, low energy consumption and long range communications. Several LPWA standards are developed, that is, long range wide area network (LoRaWAN) [5], wireless smart utility network (Wi-SUN) [6], SigFox [7], and others. These standards can be used in ISM band, especially, 920 MHz band in Japan [8], and some of them, such as LoRaWAN or Wi-SUN, are excellent in terms of usability because they can comprise a private or local network. Although this facilitates the fast and widespread diffusion of LPWAN, it will lead to an excessive concentration of end devices in the frequency band, resulting in the degradation of communication quality in the LPWAN owing to interference in the same frequency band. To avoid the degradation, techniques for confronting this interference are required.

[1] Graduate School of Engineering, Mie University, Mie, Japan.
[2] Advanced Wireless and Communication research Center (AWCC), The University of Electro-Communications, Tokyo, Japan.
[a)] narieda@pa.info.mie-u.ac.jp

DOI: 10.23919/comex.2024XBL0034
Received February 28, 2024
Accepted March 25, 2024
Publicized April 8, 2024
Copyedited June 1, 2024

Carrier sense [9] is a fundamental technique to avoid interference in the same frequency band by confirming the presence of interference before packet transmission. Carrier sense multiple access/collision avoidance (CSMA/CA) protocols are widely employed in several wireless standards such as wireless local area networks. Carrier sense requires signal detection techniques to sense interference signals. For example, the Japanese regulations for the 920 MHz band employ peak detection as the signal detection technique for carrier sense. Peak detection is a simple signal detection technique that senses target signals by utilizing the peak power in a period for signal detection. However, its signal detection capability is not superior to other signal detection techniques because of the presence of thermal noise in the end device. Energy detection [10] is also a simple signal detection technique for sensing target signals utilizing the integral value of signal energy during the period for signal detection. It can sense target signals with power near the noise floor using a signal detection period long enough to avoid the performance degradation owing to the phenomenon of signal power-to-noise ratio (SNR) walls [11, 12].

Authors have investigated carrier sense techniques based on energy detection [13] to prevent packet collisions caused by interference. In [13], although some characteristics of the energy detection based carrier sense are revealed based on theoretical and numerical analyses, the characteristics of the signal detection parameters, that is, target signal detection probability and false alarm probability, have never been revealed. It is well established that these parameters significantly affect the capabilities of signal detection and its applications [14, 15, 16]. Therefore, in this study, we investigate the effect of target false alarm probability and signal detection probability on the performance of the end device with the energy detection based carrier sense.

The remainder of this letter is organized as follows: Section 2. describes the energy detection based carrier sense. In Section 3., analytical results from the viewpoints of signal detection and wireless networks are presented. Finally, section 4. concludes this letter.

2. Energy detection based carrier sense

In [13], several characteristics of the energy detection based carrier sense are analyzed by considering the effect of the finite length of the interference packet. The signal detection probability, that is, the carrier sense success probability P_{CS} of the energy detection based carrier sense is given by

$$P_{\mathrm{CS}} = \frac{1}{N_{\mathrm{TOA}} + N_{\mathrm{CS}}} \left[2 \sum_{n=1}^{\min(N_{\mathrm{TOA}}, N_{\mathrm{CS}})} P_{\mathrm{D,A}}(n) + \left(|N_{\mathrm{TOA}} - N_{\mathrm{CS}}| + 1 \right) P_{\mathrm{D,A}} \left\{ \min(N_{\mathrm{TOA}}, N_{\mathrm{CS}}) \right\} \right], \quad (1)$$

where N_{TOA}, N_{CS}, and $\min(X, Y)$ are the numbers of samples for the interference packet, the number of samples for carrier sense, and function which provides the minimum value of X and Y, respectively. $P_{\mathrm{D,A}}(n)$ is the signal detection probability for the length of packet N_{TOA} and the carrier sense period N_{CS}, and it is expressed as follows:

$$P_{\mathrm{D,A}}(N_{\mathrm{TOA}}) = Q\left\{ \left(\frac{\mathcal{P}_{\mathrm{CS,mW}}}{\mathcal{P}_{\mathrm{N,mW}} + \min\left(1, \frac{N_{\mathrm{TOA}}}{N_{\mathrm{CS}}}\right) \mathcal{P}_{\mathrm{RX,mW}}} - 1 \right) \sqrt{N_{\mathrm{CS}}} \right\}, \quad (2)$$

where $\mathcal{P}_{\mathrm{CS,mW}}$, $\mathcal{P}_{\mathrm{N,mW}}$, $\mathcal{P}_{\mathrm{RX,mW}}$, and N_{CS} are threshold for signal detection in milliwatts, noise power in milliwatts, interference power in milliwatts, and the number of samples for signal detection, respectively. $Q(\cdot)$ [17] and $\mathcal{P}_{\mathrm{CS,mW}}$ can be expressed as,

$$Q(x) = \frac{1}{\sqrt{2}} \int_x^{\infty} e^{-t^2/2} dt, \quad (3)$$

$$\mathcal{P}_{\mathrm{CS,mW}} = \mathcal{P}_{\mathrm{N,mW}} \left\{ \frac{Q^{-1}\left(\overline{P_{\mathrm{FA}}}\right)}{\sqrt{N_{\mathrm{CS}}}} + 1 \right\}, \quad (4)$$

where $Q^{-1}(\cdot)$, $\overline{P_{\mathrm{D}}}$, and $\overline{P_{\mathrm{FA}}}$ are the inverse function of $Q(\cdot)$, target signal detection probability, and target false alarm probability, respectively. Furthermore, $\mathcal{P}_{\mathrm{N,dBm}} = 10\log_{10}\left(\mathcal{P}_{\mathrm{N,mW}}/1\,\mathrm{mW}\right)$ can be expressed as [18]

$$\mathcal{P}_{\mathrm{N,dBm}} = -174 + 10\log_{10}(BW) + NF, \quad (5)$$

where BW and NF are the channel bandwidth and noise figure, respectively.

Figure 1 shows the characteristics of $\mathcal{P}_{\mathrm{CS}}$ for different $T_{\mathrm{TOA}} = 51.5\,\mathrm{ms}$, 102.7 ms, 153.9 ms, where T_{TOA} is a time on air of the packet. The results shown in Fig. 1 are obtained for $BW = 200\,\mathrm{kHz}$, $NF = 6\,\mathrm{dB}$, and $\mathcal{P}_{\mathrm{RX,dBm}} = 10\log_{10}\left(\mathcal{P}_{\mathrm{RX,mW}}/1\mathrm{mW}\right) = -125\,\mathrm{dBm}$. The parameter values of BW and NF are also employed in this section as well as in the next section. Note that carrier sense periods T_{CS} in ms for carrier sense levels $\mathcal{P}_{\mathrm{CS,dBm}} = -127.5\,\mathrm{dBm}$, $-125\,\mathrm{dBm}$, $-122.5\,\mathrm{dBm}$ are $T_{\mathrm{CS}} = 18.18\,\mathrm{ms}$, 6.00 ms, 2.04 ms, respectively. As shown in Fig. 1, the characteristics of signal detection probability deteriorate as T_{TOA} decreases. This is because the interference signals do not occupy the carrier sense period owing to the finite packet length and carrier sense period, resulting in degraded accuracy of the energy detection based carrier sense. Note that the details of the characteristics are presented in [13]. In addition, two peaks in the characteristic can be observed as shown in Fig. 1, and it can be seen that the right-peaks of the characteristic are nearly the same at the around $\mathcal{P}_{\mathrm{CS,dBm}} = -125\,\mathrm{dBm}$. The right-peak of the characteristic is more important than the left-peak, because the carrier sense period at the right-peak is less than that at the left-peak, even though the characteristics are nearly the same.

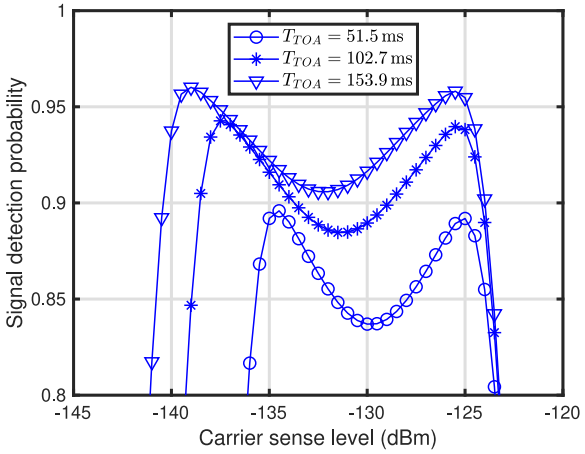

Fig. 1 Signal detection probability for carrier sense levels. $T_{\mathrm{TOA}} = 51.5\,\mathrm{ms}$, 102.7 ms, 153.9 ms, $\overline{P_{\mathrm{D}}} = 0.99$, $\overline{P_{\mathrm{FA}}} = 0.01$, $BW = 200\,\mathrm{kHz}$, $NF = 6\,\mathrm{dB}$, and $\mathcal{P}_{\mathrm{RX,dBm}} = -125\,\mathrm{dBm}$. Note that carrier sense period for $\mathcal{P}_{\mathrm{CS,dBm}} = -127.5\,\mathrm{dBm}$, $-125\,\mathrm{dBm}$, $-122.5\,\mathrm{dBm}$ are $T_{\mathrm{CS}} = 18.18\,\mathrm{ms}$, 6.00 ms, 2.04 ms, respectively.

3. Numerical examples based analyses

3.1 Effect of $\overline{P_{\mathrm{D}}}$ and $\overline{P_{\mathrm{FA}}}$ on performance of energy detection based carrier sense

First, we present the characteristics of the energy detection based carrier sense for several $\overline{P_{\mathrm{D}}}$ and $\overline{P_{\mathrm{FA}}}$. Figure 2 shows the characteristics of the signal detection probability for $\overline{P_{\mathrm{D}}} = 0.99$, $\overline{P_{\mathrm{FA}}} = 0.1$, 0.04, 0.01, 0.004, 0.001, and $\mathcal{P}_{\mathrm{RX,dBm}} = -125\,\mathrm{dBm}$. As shown in Fig. 2, the signal detection probability of $\overline{P_{\mathrm{FA}}} = 0.1$ outperforms that of $\overline{P_{\mathrm{FA}}} = 0.04$ to $\overline{P_{\mathrm{FA}}} = 0.001$. From the results, it can be seen that the characteristics of the signal detection probability are degraded as $\overline{P_{\mathrm{FA}}}$ decreases, and the carrier sense levels on the right-peak of the characteristics do not change for any $\overline{P_{\mathrm{FA}}}$. Figure 3 shows the characteristics of the signal detection probability for $\overline{P_{\mathrm{D}}} = 0.9$, 0.99, 0.999, $\overline{P_{\mathrm{FA}}} = 0.1$, 0.01, and $\mathcal{P}_{\mathrm{RX,dBm}} = -125\,\mathrm{dBm}$. As shown in Fig. 3, the right-peaks of the characteristics shift to the right as $\overline{P_{\mathrm{D}}}$ increases. This leads to a difference in the signal detection probability

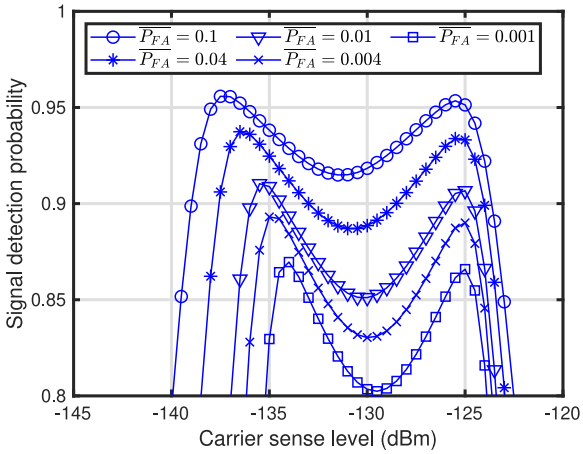

Fig. 2 Signal detection probability for carrier sense levels. $T_{\mathrm{TOA}} = 61.7\,\mathrm{ms}$, $\mathcal{P}_{\mathrm{RX,dBm}} = -125\,\mathrm{dBm}$, $\overline{P_{\mathrm{D}}} = 0.99$, and $\overline{P_{\mathrm{FA}}} = 0.1$, 0.04, 0.01, 0.004, 0.001.

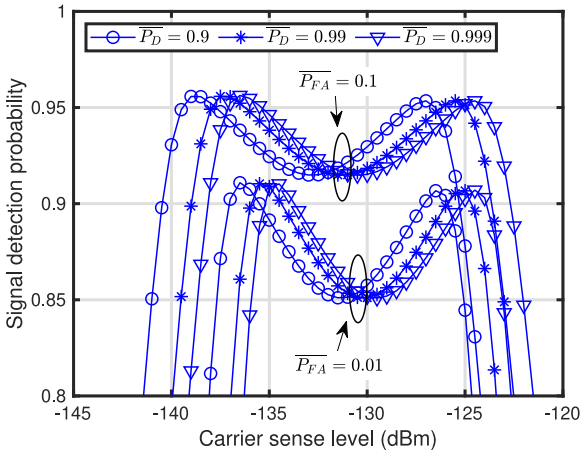

Fig. 3 Signal detection probability for carrier sense levels. T_{TOA} = 61.7 ms, $\mathcal{P}_{\mathrm{RX,dBm}} = -125$ dBm, $\overline{P_{\mathrm{FA}}} = 0.1, 0.01$ and $\overline{P_{\mathrm{D}}} = 0.9, 0.99, 0.999$.

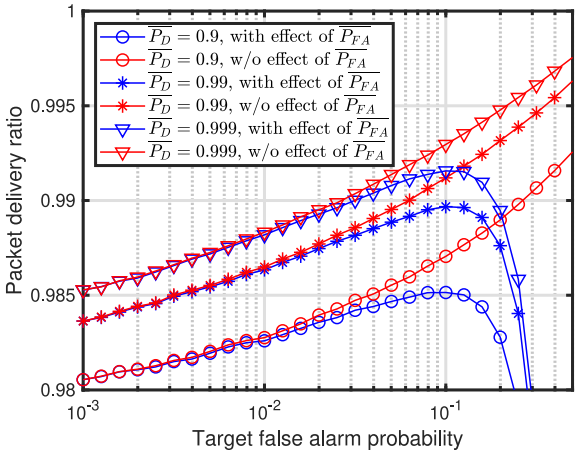

Fig. 4 Packet delivery ratio for $\overline{P_{\mathrm{FA}}}$s. $\mathcal{P}_{\mathrm{CS,dBm}} = -125$ dBm and $\overline{P_{\mathrm{D}}} = 0.9$, 0.99, 0.999.

Table I Parameters for discussion based on the approach from the viewpoint of wireless network

Parameters	Variable	Value
p.d.f. of end device distribution	-	Uniform distribution
Number of end devices	-	200
Radius of communication area	-	1500 m
Path loss exponent (end device → gateway)	-	2.7
Path loss exponent (end device ↔ end device)	-	3.3
Transmit power	-	13 dBm
Packet length	T_{TOA}	61.7 ms
Spreading factor	-	7
Average transmission period (Poisson distribution)	T_{S}	180 sec
Maximum trial times for packet transmission	-	3

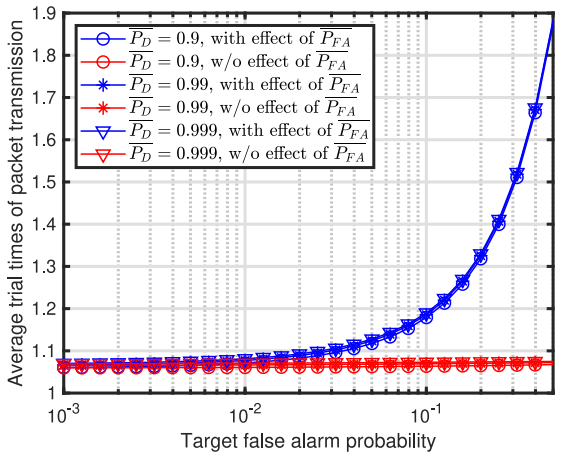

Fig. 5 Average trial times of packet transmission for $\overline{P_{\mathrm{FA}}}$s. $\mathcal{P}_{\mathrm{CS,dBm}} = -125$ dBm and $\overline{P_{\mathrm{D}}} = 0.9, 0.99, 0.999$.

at the carrier sense level.

The results presented in this subsection clearly lead to a better carrier sense success probability with the highest possible $\overline{P_{\mathrm{FA}}}$. However, the results are derived only from the viewpoint of signal detection and lacked the results from the viewpoint of wireless networks. Hence, in the next subsection, we discuss this approach from the viewpoint of signal detection and wireless networks.

3.2 Effect of $\overline{P_{\mathrm{FA}}}$ on performance of end devices with energy detection based carrier sense

Table I lists the parameters for the discussion based on the approach from the viewpoint of wireless networks, and numerical examples are presented. As a simple network model, LoRaWAN with a single spreading factor is employed. The networks have a communication area with a radius of 1500 m and comprise 200 end devices and one gateway. Each end device is geographically deployed in the area according to a uniform distribution. The path loss exponents for radiowave propagation in the network are employed at 2.7 and 3.3 for the end device to the gateway and the end device to the end device, respectively. Each end device transmits its data in packets of $T_{\mathrm{TOA}} = 61.7$ ms in length with transmit power 13 dBm, and the average transmission period is $T_{\mathrm{S}} = 180$ s according to Poisson distribution. Furthermore, a maximum trial times for packet transmission is 3.

Figure 4 shows the packet delivery ratio of $\overline{P_{\mathrm{FA}}}$. In Fig. 4, the characteristics of packet delivery ratio with and without the effect of $\overline{P_{\mathrm{FA}}}$ are presented for $\overline{P_{\mathrm{D}}} = 0.9, 0.99, 0.999$. Note that the effect of $\overline{P_{\mathrm{FA}}}$ here indicates that the end device cannot transmit packets owing to $\overline{P_{\mathrm{FA}}}$ when no arrival interference. As shown in Fig. 4, the characteristic with the effect of $\overline{P_{\mathrm{FA}}}$ exhibit a peak at approximately $\overline{P_{\mathrm{FA}}} = 0.1$. The result is caused by the behavior of the energy detection based carrier sense at the end device when no interference existed. Figure 5 shows average trial times of packet transmission. As shown in Fig. 5, the characteristics with the effect of $\overline{P_{\mathrm{FA}}}$ are greater than those without the effect of $\overline{P_{\mathrm{FA}}}$ as $\overline{P_{\mathrm{FA}}}$ increases. From these results, it can be seen that the end device misidentifies the presence of interference owing to a high $\overline{P_{\mathrm{FA}}}$; therefore, each end device is prone to losing the packet transmission opportunity. These results lead to the presence of an optimal $\overline{P_{\mathrm{FA}}}$. In addition, Fig. 6 shows the characteristics of the signal detection probability at the end device when there are interferences for $\overline{P_{\mathrm{D}}} = 0.9, 0.99, 0.999$. As shown in Fig. 6, the characteristics of the signal detection probability increases as $\overline{P_{\mathrm{D}}}$ and $\overline{P_{\mathrm{FA}}}$ increase, because of the characteristics as shown in Figs. 2 and 3. The result solidifies the discussion of the characteristics shown

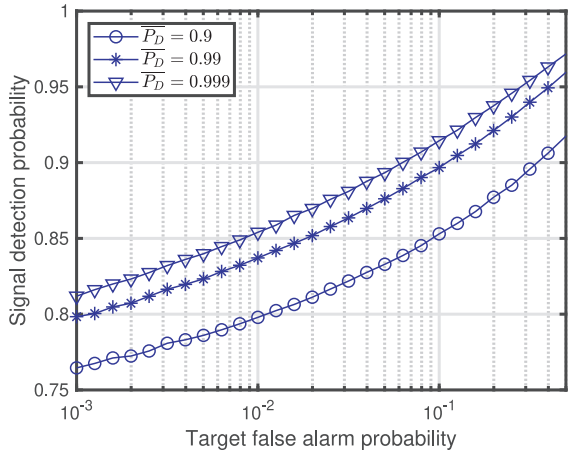

Fig. 6 Signal detection probability for $\overline{P_{\mathrm{FA}}}$s. $\mathcal{P}_{\mathrm{CS,dBm}} = -125$ dBm and $\overline{P_{\mathrm{D}}} = 0.9, 0.99, 0.999$.

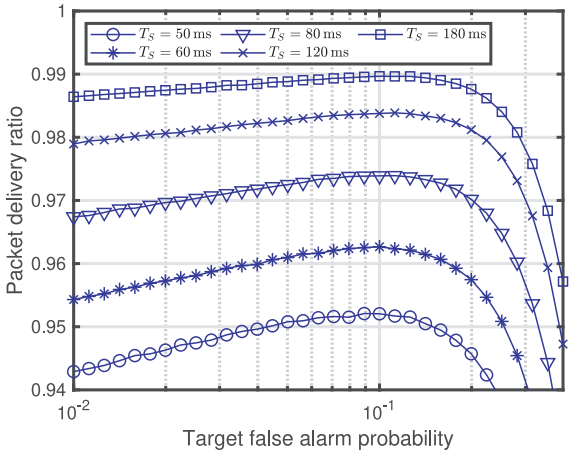

Fig. 7 Packet delivery ratio for $\overline{P_{\mathrm{FA}}}$s. $\mathcal{P}_{\mathrm{CS,dBm}} = -125$ dBm, $\overline{P_{\mathrm{D}}} = 0.99$, and $T_{\mathrm{S}} = 50$ ms, 60 ms, 80 ms, 120 ms, 180 ms.

in Fig. 4 because the packet delivery ratio shown in Fig. 4 deteriorates for approximately $\overline{P_{\mathrm{FA}}} > 0.1$, despite of the good signal detection probability.

Finally, Fig. 7 shows the packet delivery ratio for different T_{S}. As shown in Fig. 7, the optimal $\overline{P_{\mathrm{FA}}}$ value decreases as T_{S} increases. This is because it decreases the case with no interference during the carrier sense period by increasing T_{S}, and it can be seen that T_{S} depends on the optimal value of $\overline{P_{\mathrm{FA}}}$.

4. Conclusion

This study investigated signal detection parameters, such as the target signal detection probability and target false alarm probability, of the energy detection based carrier sense in LPWAN. The characteristics of aforementioned target probabilities in the energy detection based carrier sense were discussed based on the approaches from the viewpoint of signal detection and wireless network. Numerical example based analyses revealed that the characteristics that target false alarm probability must be optimized to enhance the performance of the end device with the energy detection based carrier sense.

Acknowledgment

This research and development work was supported by the MIC/SCOPE #JP215006001.

References

[1] S. Mumtaz, A. Alsohaily, Z. Pang, A. Rayes, K.F. Tsang, and J. Rodriguez, "Massive internet of things for industrial applications: Addressing wireless iot connectivity challenges and ecosystem fragmentation," *IEEE Ind. Electron. Mag.*, vol. 11, no. 1, pp. 28–33, Jan. 2017. DOI: 10.1109/mie.2016.2618724

[2] J. Botero-Valencia, L. Castano-Londono, D. Marquez-Viloria, and M. Rico-Garcia, "Data reduction in a low-cost environmental monitoring system based on LoRa for WSN," *IEEE Internet Things J.*, vol. 6, no. 2, pp. 3024–3030, 2019. DOI: 10.1109/jiot.2018.2878528

[3] M. Rizzi, P. Ferrari, A. Flammini, and E. Sisinni, "Evaluation of the IoT LoRaWAN solution for distributed measurement applications," *IEEE Trans. Instrum. Meas.*, vol. 66, no.12, pp. 3340–3349, Dec. 2017. DOI: 10.1109/tim.2017.2746378

[4] U. Raza, P. Kulkami, and M. Sooriyabandara, "Low power wide area networks: An overview," *IEEE Commun. Surveys Tuts.*, vol. 19, no. 2, pp. 855–873, 2017. DOI: 10.1109/comst.2017.2652320

[5] LoRa Alliance, https://lora-alliance.org/, accessed March 17, 2022.

[6] P. Beecher, "Comparing IoT networks at a glance," Wi-SUN Alliance, San Ramon, CA, USA, White Paper, https://www.wi-sun.org/wp-content/uploads/Wi-SUN-Alliance-Comparing_IoT_Networks-r1.pdf, Dec. 2017, accessed May 28, 2021.

[7] Sigfox-The Global Communication Service Provider for the Internet of Things (IoT), https://www.sigfox.com/en, accessed March 17, 2022.

[8] ARIB STD-T108, v. 1.2, "Association of radio industiries and businesses," Jan. 2018 (in Japanese).

[9] L. Kleinrock and F. Tobagi, "Packet switching in radio channels: Part I - Carrier sense multiple-access modes and their throughput-delay characteristics," *IEEE Trans. Commun.*, vol. 23, no. 12, pp. 1400–1416, 1975. DOI: 10.1109/tcom.1975.1092768

[10] H. Urkowitz, "Energy detection of unknown deterministic signals," *Proc. IEEE*, vol. 55, no. 4, pp. 523–531, 1967. DOI: 10.1109/proc.1967.5573

[11] R. Tandra and A. Sahai, "SNR walls for signal detection," *IEEE J. Sel. Topics Signal Process.*, vol. 2, no. 1, pp. 4–17, 2008. DOI: 10.1109/jstsp.2007.914879

[12] A. Mariani, A. Giorgetti, and M. Chiani, "Effects of noise power estimation on energy detection for cognitive radio applications," *IEEE Trans. Commun.*, vol. 59, no. 12, pp. 3410–3420, 2011. DOI: 10.1109/tcomm.2011.102011.100708

[13] S. Narieda and T. Fujii, "Energy detection based carrier sense in LPWAN," *IEEE Access*, vol. 11, pp. 79105–79119, 2023. DOI: 10.1109/access.2023.3299219

[14] D.-J. Lee and M.-S. Jang, "Optimal spectrum sensing time considering spectrum handoff due to false alarm in cognitive radio networks," *IEEE Commun. Lett.*, vol. 13, no. 12, pp. 899–901, 2009. DOI: 10.1109/lcomm.2009.12.091448

[15] R.C.D.V. Bomfin, D.A. Guimarães, and R.A.A. de Souza, "On the probability of false alarm of the power spectral density split cancellation method," *IEEE Wireless Commun. Lett.*, vol. 5, no. 2, pp. 164–167, 2016. DOI: 10.1109/lwc.2015.2514104

[16] B.J.B. Fonseca, "Simple bounds for the probability of false alarm to design sensor detection systems using the scan statistic," *IEEE Trans. Signal Inform. Process. Netw.*, vol. 5, no. 1, pp. 70–85, 2019. DOI: 10.1109/tsipn.2018.2854634

[17] J.G. Proakis, *Digital Communications*, 4th ed., McGraw-Hill, 2001.

[18] B. Razavi, *RF Microelectronics*, 2nd edition., Prentice Hall, 2012.